

Original Article

Intraspecific variation in multiple trait responses of *Alexandrium ostenfeldii* towards elevated $p\text{CO}_2$

Karen M. Brandenburg^{a,b,*}, Bernd Krock^c, Helena C.L. Klip^{a,b,d}, Appy Sluijs^b,
Paolina Garbeva^e, Dedmer B. Van de Waal^a

^a Department of Aquatic Ecology, Netherlands Institute of Ecology (NIOO-KNAW), Droevendaalsesteeg 10, 6708 PB Wageningen, Netherlands

^b Department of Earth Sciences, Faculty of Geosciences, Utrecht University, Princetonlaan 8a, 3584 CB Utrecht, Netherlands

^c Section Ecological Chemistry, Alfred Wegener Institut-Helmholtz Zentrum für Polar- und Meeresforschung (AWI), Am Handelshafen 12, 27570 Bremerhaven, Germany

^d Section Shelf Sea System Ecology, Alfred Wegener Institut-Helmholtz Zentrum für Polar- und Meeresforschung (AWI), Biologische Anstalt Helgoland (BAH), Kurpromenade 201, 27498 Helgoland, Germany

^e Department of Microbial Ecology, Netherlands Institute of Ecology (NIOO-KNAW), Droevendaalsesteeg 10, 6708PB Wageningen, Netherlands

ARTICLE INFO

Keywords:

Ocean acidification
Phenotypic plasticity
Harmful algal blooms
Alexandrium ostenfeldii

ABSTRACT

Dissolved oceanic CO_2 concentrations are rising as result of increasing atmospheric partial pressure of CO_2 ($p\text{CO}_2$), which has large consequences for phytoplankton. To test how higher CO_2 availability affects different traits of the toxic dinoflagellate *Alexandrium ostenfeldii*, we exposed three strains of the same population to 400 and 1,000 $\mu\text{atm CO}_2$, and measured traits including growth rate, cell volume, elemental composition, ^{13}C fractionation, toxin content, and volatile organic compounds (VOCs). Strains largely increased their growth rates and particulate organic carbon and nitrogen production with higher $p\text{CO}_2$ and showed significant changes in their VOC profile. One strain showed a significant decrease in both PSP and cyclic imine content and thereby in cellular toxicity. Fractionation against ^{13}C increased in response to elevated $p\text{CO}_2$, which may point towards enhanced CO_2 acquisition and/or a downscaling of the carbon concentrating mechanisms. Besides consistent responses in some traits, other traits showed large variation in both direction and strength of responses towards elevated $p\text{CO}_2$. The observed intraspecific variation in phenotypic plasticity of important functional traits within the same population may help *A. ostenfeldii* to negate the effects of immediate environmental fluctuations and allow populations to adapt more quickly to changing environments.

1. Introduction

The atmospheric partial pressure of CO_2 ($p\text{CO}_2$) is increasing at an exceptional rate due to anthropogenic activities (Hönisch et al., 2012; Stocker et al., 2013). The oceans act as the world's largest exogenic carbon reservoir and will take up more CO_2 as atmospheric concentrations rise (Post et al., 1990; Riebesell et al., 2009). This will result in a change in the speciation of dissolved inorganic carbon (DIC) in the upper ocean layer, and a subsequent drop in pH values. This ocean acidification is expected to have considerable consequences for marine life (Doney et al., 2009; Dutkiewicz et al., 2015; Falkowski et al., 1998; Hurd et al., 2020). Specifically for organisms living in the surface layer of the oceans, such as phytoplankton, that utilize CO_2 for photosynthesis (Beardall et al., 2009).

Phytoplankton vary in their inorganic carbon (C) acquisition due to

differences in the operation of carbon concentrating mechanisms (CCMs; Giordano et al., 2005). These CCMs are responsible for increasing the concentration of CO_2 in the vicinity of Ribulose-1,5-bisphosphate carboxylase/oxygenase (RubisCO) to ensure effective carboxylation (Badger et al., 1998; Thoms et al., 2001), and include active CO_2 and HCO_3^- uptake, the use of carbonic anhydrase (CA) to accelerate the interconversion between CO_2 and HCO_3^- , and minimization of CO_2 efflux (leakage) from the cell (Giordano et al., 2005; Reinfelder, 2011). Dinoflagellates possess the very inefficient type II RubisCO, which among all eukaryotic phytoplankton exhibits the lowest affinity for its substrate CO_2 (Badger et al., 1998; Morse et al., 1995). However, studies suggest that dinoflagellates are not C limited at present atmospheric CO_2 levels due to the operation of effective CCMs (Eberlein et al., 2014; Fu et al., 2008; Ratti et al., 2007; Rost et al., 2006; Van de Waal et al., 2019). They could nonetheless benefit from higher CO_2 concentrations by

* Corresponding author.

E-mail address: k.brandenburg@nioo.knaw.nl (K.M. Brandenburg).

<https://doi.org/10.1016/j.hal.2020.101970>

Received 22 July 2020; Received in revised form 18 November 2020; Accepted 11 December 2020

1568-9883/© 2020 The Authors. Published by Elsevier B.V. This is an open access article under the CC BY license (<http://creativecommons.org/licenses/by/4.0/>).

downscaling their CCMs and reallocate energy and resources towards other cellular processes (Rost et al., 2008; Van de Waal and Litchman, 2020).

Alterations in oceanic carbonate chemistry could thus lead to changes in the expression of various phytoplankton functional traits. For instance, nitrogen (N) limitation combined with elevated $p\text{CO}_2$ resulted in reduced N stress in *Alexandrium fundyense* and *Scrippsiella trochoidea* presumably due to reallocation of energy from C to N assimilation as a consequence of lowered costs of C acquisition (Eberlein et al., 2016). Moreover, growth rates and toxicity increased in response to elevated $p\text{CO}_2$ in dinoflagellate species *Karodinium veneficum* and *A. catenella* (Fu et al., 2008; Tatters et al., 2013). In contrast, unaltered growth rates and a decrease in cellular toxicity were observed for two strains of *A. fundyense* due to higher CO_2 concentrations (Van de Waal et al., 2014). Trait responses may also vary within populations, as several *A. ostenfeldii* strains from the Baltic Sea responded differently to CO_2 in experiments (Kremp et al., 2012). Slower growing strains generally showed an increase in growth rate, while faster growing strains did not respond or responded negatively. However, alterations in toxin production were more consistent, as all tested strains increased their toxicity through higher saxitoxin (STX) production (Kremp et al., 2012).

Phytoplankton, including dinoflagellates, may also emit volatile organic compounds (VOCs; Fink, 2007; Lawson et al., 2019; Zuo, 2019). These are compounds of low molecular weight, well known as swift infochemicals in both aquatic and terrestrial ecosystems (Schmidt et al., 2015), and may play a variety of roles in phytoplankton metabolism and ecology. For instance, these compounds may help in grazer defense and interactions with other micro-organisms (Fink, 2007), or can be important in relieving abiotic stress and protection against pathogens (Shiojiri et al., 2006; Sunda et al., 2002). VOCs are thought to be produced during active growth (Buchan et al., 2014) and can be regulated by changes in abiotic conditions, such as light and nutrient availability (Bromke et al., 2013; Halsey et al., 2017) or microbial interactions (Schmidt et al., 2015). We expect that elevated $p\text{CO}_2$ will increase C assimilation and, consequently, increase VOC synthesis, as VOCs are C-rich compounds that comprise a significant part of the dissolved organic carbon pool (Hauser et al., 2013; Ruiz-Halpern et al., 2010). The overall regulation of VOCs is referred to as the ‘volatilome’, which has been shown to vary across phytoplankton species (Lawson et al., 2019). It is still unclear whether the volatilome may also vary across strains.

Harmful algal bloom (HAB)-forming species, and specifically dinoflagellates, are known to possess a high genetic and phenotypic variation within populations, and this is thought to contribute to their success (Alpermann et al., 2010; Brandenburg et al., 2018; Burkholder and Glibert, 2006; Godhe et al., 2016; Maranda et al., 1985; Medlin et al., 2000). Functional trait variation within populations enhances complementarity of traits, which can result in higher resource use efficiencies, enhanced resistance to consumers, and resilience to environmental changes (Bolnick et al., 2011; Hooper et al., 2005; Violle et al., 2012). In addition to standing variation in populations that is mainly beneficial for the longer term selection and adaptation (Barrett and Schluter, 2008), phenotypic plasticity in trait responses can buffer the immediate effects of environmental fluctuations and allow individual strains to persist by widening their ecological niche (Charmantier et al., 2008; Litchman et al., 2012). Strains may differ in their trait plasticity ranges, where low trait plasticity can reflect stronger specialization under more stable environmental conditions, while higher plasticity may be favorable in dynamic environments (Nicotra et al., 2010), as is the case during the development of HABs.

Here, we assess how the regulation of various functional traits changes in response to elevated $p\text{CO}_2$ in three strains of *A. ostenfeldii* derived from a single population. *A. ostenfeldii* is a notorious producer of various neurotoxins, including paralytic shellfish poisoning (PSP) toxins, and cyclic imine toxins, such as gymnodimines (GYM) and spirolides (SPX; Cembella et al., 2000). *A. ostenfeldii* usually occurs in low background numbers in phytoplankton assemblages, though blooms of

this species have become more prominent in recent years (Borkman et al., 2012; Burson et al., 2014; Kremp et al., 2009; Tomas et al., 2012). The three studied strains were isolated from a small creek in the Netherlands, where dense blooms annually recur since 2012 (Brandenburg et al., 2017; Burson et al., 2014; Van de Waal et al., 2015). Microsatellite analysis of this population revealed that strains were genetically very similar, presumably due to a geographical bottleneck effect, but possessed considerable phenotypic trait variation (Brandenburg et al., 2018). Consequently, we also expect some intraspecific variation in trait responses to alterations in carbonate chemistry. Tested traits included growth rate, cell size, elemental composition, toxin content, ^{13}C fractionation, and untargeted VOC production.

2. Material & methods

2.1. Culturing

The three *Alexandrium ostenfeldii* strains (AON13, AON15, AON5.26) used in this experiment were isolated from the Ouwerkerkse Kreek, the Netherlands (51°62'N, 399°E), a brackish water creek, during summer blooms in 2015 (AON5.26) and 2016 (AON13; AON15). Cultures of these strains were kept in $\frac{1}{2}\text{K}$ – medium (after Keller et al., 1987), using 0.2 μm sterilized North Sea water adjusted to a salinity of 10 by dilution with demineralized water. Prior to the experiment, culture medium was pre-aerated with air containing $p\text{CO}_2$ of 400 μatm (ambient CO_2 treatment) and 1000 μatm (high CO_2 treatment). These concentrations were obtained by mixing pressurized air with CO_2 (100%) using mass flow controllers (SLA5800 series, Brooks Instruments, Hatfield, US). CO_2 concentrations were verified by a nondispersive infrared analyzer system (LI-820, LI-COR Biosciences, Bad Homburg, Germany). Before the start of the experiment, cultures were first acclimated to the experimental CO_2 concentrations for 14 days, representing at least 3 generations. Cultures were subsequently inoculated with densities of ~ 400 cells mL^{-1} and grown in 2 L round bottom flasks in triplicates, at a temperature of 18 °C and an incident light intensity of 85 $\mu\text{mol photons m}^{-2}\text{s}^{-1}$, with a light dark cycle of 16:8 h. Every other day, samples for assessing carbonate chemistry and cell densities were taken. After at least 3 generations, cultures were harvested in exponential growth phase at densities of approximately 4.0×10^3 cells mL^{-1} for the assessment of elemental composition, toxin content, ^{13}C fractionation, and untargeted VOC analysis as described below.

2.2. Carbonate chemistry

The pH of the cultures was measured every other day using a 2-point calibrated pH meter (Multi 350i, WTW, Weilheim, Germany). Samples for dissolved inorganic carbon (DIC) were taken simultaneously over the course of the experiment and analyzed with a TIC/TOC analyzer (TOC-LCPH FA, E200 Total Organic Carbon Analyser; ASI-L Autosampler, Shimadzu, Kyoto, Japan). The carbonate chemistry was subsequently calculated with CO_2sys (Pierrot et al., 2006) using pH_{NBS} (National Bureau of Standards) and DIC of each time point. Equilibrium constants of Mehrbach et al. (1973), refitted by Dickson and Millero (1987) were chosen.

2.3. Growth rate and cell size

Cell densities were estimated by taking a sample for cell counts every other day. A sample of 5 mL was taken and fixed with Lugol’s iodine solution (Lugol) to a final concentration of 1% and stored in the dark at 4 °C until analysis. 1 mL aliquots of sample were subsequently counted on an inverted microscope (DMI 4000B; Leica Microsystems CMS GmbH, Mannheim, Germany), this was done in triplicate for samples from the harvest day. Specific growth rates (μ) were calculated for each replicate of each strain by fitting an exponential function through all cell counts over time, following:

$$N_t = N_0 \exp^{\mu t}$$

where N_t refers to the cell concentrations at time t , and N_0 to the cell concentrations at the start of each experiment.

Lugol fixed samples from the harvest day were used for cell size measurements (diameter) with an inverted microscope (DMI 4000B; Leica Microsystems CMS GmbH, Mannheim, Germany), and software Cell'D (Imaging software for Life Sciences Microscopy, Olympus, Tokyo, Japan). The diameter data was then used to calculate cell volume assuming an ellipsoid shape. For each replicate, at least 100 cells were measured.

2.4. Elemental composition

Particulate organic carbon (POC), particulate organic nitrogen (PON) and particulate organic phosphorus (POP) were determined in 20–40 mL of culture material collected on a pre-combusted glass microfiber filter (Whatman GF/F, Maidstone, UK). Filters were dried overnight at 60 °C and stored in the dark until further analyses. For POC and PON analyses, and $\delta^{13}\text{C}_{\text{POC}}$, a subsample (14%) of every filter was punched out and folded into a tin cup (as a whole filter does not fit into the cups) and analyzed on an elemental analyzer (Flash 2000, Thermo Scientific, Karlsruhe, Germany) coupled to an isotope ratio mass spectrometer (IRMS, Thermo Scientific, Karlsruhe, Germany; [Morrién et al., 2017](#)). $\delta^{13}\text{C}_{\text{POC}}$ was reported relative to the Vienna PeeDee Belemnite standard (VPDB). POP was analyzed by first combusting the remainder of the filter (86%) for 30 min at 550 °C in Pyrex glass tubes, followed by a digestion step with 5 mL persulfate (2.5%) for 30 min at 120 °C. This digested solution was measured for PO_4^{3-} on a QuAAtro39 AutoAnalyzer (SEAL Analytical Ltd., Southampton, UK).

2.5. Toxin sampling and analyses

Samples for toxin analyses (PSP toxins and cyclic imines) were taken by filtration of 20–40 mL of *A. ostentfeldii* culture over glass microfiber filters (GF/F, Whatman, Maidstone, UK), which were stored at –20 °C until further analysis. PSP toxins were determined by ion pair liquid chromatography coupled to post-column derivatization and fluorescence detection, as described in [Krock et al. \(2007\)](#) and [Van de Waal et al. \(2015\)](#). The cyclic imine toxin measurements (SPX and GYM) were performed on a 1100 LC liquid chromatograph (Agilent, Waldbronn, Germany) coupled to a 4000 Q Trap triple-quadrupole mass spectrometer (SCIEX, Darmstadt, Germany) with a Turbo V ion source. Toxins were quantified by external calibration curves of SPX-1 and GYM A with standard solutions ranging from 10 to 1000 pg μL^{-1} , each. Other SPXs and GYMs for which no standards are available were calibrated against the SPX-1 and GYM A calibration curve, respectively, and expressed as SPX-1 or GYM A equivalents. For further details, also see [Van de Waal et al. \(2015\)](#).

2.6. ^{13}C fractionation

For isotopic measurements of the dissolved inorganic carbon ($\delta^{13}\text{C}_{\text{DIC}}$), every other day 4 mL of culture suspension was filtered through sterile 0.2 μm cellulose acetate filters (VWR International, Amsterdam, the Netherlands) and stored at 4 °C. 0.7 mL of the filtrate was then transferred to 8 mL vials, which contained three drops of 102% H_3PO_4 solution, and headspaces filled with helium. After equilibration, the isotopic composition in the headspace was measured using a Gas-Bench-II coupled to a Thermo Delta-V advantage isotope ratio mass spectrometer, with a precision of $\pm 0.1\%$. ^{13}C fractionation (ϵ_p) was calculated relative to the isotopic composition of dissolved CO_2 in the water ($\delta^{13}\text{C}_{\text{CO}_2}$) with an equation modified after [Freeman and Hayes \(1992\)](#):

$$\epsilon_p = \frac{(\delta^{13}\text{C}_{\text{CO}_2} - \delta^{13}\text{C}_{\text{POC}})}{\left(1 + \frac{\delta^{13}\text{C}_{\text{POC}}}{1000}\right)}$$

In order to calculate the isotopic composition of CO_2 ($\delta^{13}\text{C}_{\text{CO}_2}$) from $\delta^{13}\text{C}_{\text{DIC}}$, we calculated the isotopic composition of HCO_3^- ($\delta^{13}\text{C}_{\text{HCO}_3^-}$) based on $\delta^{13}\text{C}_{\text{DIC}}$ according to a mass balance relation following [Zeebe and Wolf-Gladrow \(2001\)](#) and the temperature-dependent fractionation factors between CO_2 and HCO_3^- and CO_3^{2-} and HCO_3^- , as determined by [Mook et al. \(1974\)](#) and [Zhang et al. \(1995\)](#), respectively.

2.7. VOC analysis

Volatile organic compounds (VOCs) were measured at the harvest day of each experiment. 75 mL of culture from each replicate was transferred to sterile flasks and two Rotilabo®-silicone tubes (PDMS tubes; Carl Roth GmbH+Co. KG, Karlsruhe, Germany) were added to each flask for collecting VOCs. The PDMS tubes were pretreated as described by [Kallenbach et al. \(2015\)](#). The tubes were incubated with the cultures for exactly 20 min, after which they were removed and kept at –20 °C until further analysis.

VOCs were desorbed from the PDMS tubes by using an automated thermodesorption unit (model UnityTD-100, Markes International Ltd., UK) at 250 °C for 12 min (He flow 50 mL min^{-1}). The desorbed VOCs were subsequently collected on a cold trap at –10 °C and introduced into the GC-QTOF (model Agilent 7890B GC and the Agilent 7200AB QTOF, USA) by heating the cold trap for 10 min to 280 °C. The column used was a 30 \times 0.25 mm ID DB-5MS with as film thickness of 0.25 μm (Agilent 122–5532, USA). The temperature program was as follows: 2 min. at 39 °C, 3.5 °C min^{-1} to 95 °C, 4 °C min^{-1} to 165 °C and finally 15 °C min^{-1} to 280 °C that was held for 15 min. VOCs were detected by the MS operating at 70 eV in EI mode. Mass spectra were acquired in full scan mode (30–400 AMU, 4 spectra s^{-1}). The collected GC/MS data were subsequently converted to mzData files using the Chemstation B.06.00 (Agilent Technologies, Santa Clara, USA) and further processed (peak picking, baseline correction and peak alignment) in an untargeted manner using MZmine V2.14.2 ([Schulz-Bohm et al., 2015](#); [Tyc et al., 2015](#)).

2.8. Statistical analyses

Statistical analyses were performed in R version 3.6.3 ([R Core Team 2018](#)). A generalized linear model (glm) was fitted to the each of the measured traits including fixed effects for CO_2 and strain, and an interaction effect between strain and CO_2 to assess significant responses. Data was checked for normality and residuals were checked for heteroscedasticity. Pairwise comparisons (following the Tukey method) between the two CO_2 treatments and between the three strains were made to assess significant differences in the traits using the R package “emmeans” ([Lenth et al., 2020](#)). We also tested whether the strains responded differently to elevated $p\text{CO}_2$ by comparing their response to each of the measured traits using the “contrast” function from the R package “emmeans”.

The significance of the relationship between ^{13}C fractionation and the concentration of CO_2 in the water, and POC production/ $[\text{CO}_2]$ was tested using linear model and a hyperbolic regression following [Hoins et al. \(2015\)](#), respectively.

Multivariate analysis of processed and normalized (log transformation and mean centered) GC–MS data was conducted with MetaboAnalyst 3.0 (<http://www.metaboanalyst.ca/MetaboAnalyst>, [Xia et al., 2015](#)), where we used a partial least squares discriminant analysis (PLS-DA) using the R package “mixOmics” to illustrate the differences in the mass traces of VOCs produced by the strains and between CO_2 treatments ([Rohart et al., 2017](#)).

3. Results

3.1. Experiment control

The carbonate chemistry between the ambient and high CO₂ treatments was significantly different for all three strains during the experiment (Table 1; $P < 0.001$), despite a drift in pH due to biomass build-up. Specifically, mean $p\text{CO}_2$ ranged between 213 and 357 μatm in the ambient CO₂ treatments, and between 479 and 676 μatm in the high CO₂ treatments.

3.2. Comparison between strains

Several differences between the strains were apparent in the ambient CO₂ treatments. For instance, AON13 grew at $0.17 \pm 0.008 \text{ d}^{-1}$, which was significantly slower than the two other strains, AON15 and AON5.26, that had average growth rates of 0.22 ± 0.01 and $0.22 \pm 0.006 \text{ d}^{-1}$, respectively (Fig. 1a; $P < 0.001$). Toxin contents also varied between the strains, with significantly different cyclic imine toxin contents of 4.25, 5.74 and 3.02 pg cell^{-1} , for AON13, AON15 and AON5.26, respectively (Fig. 1b; $P < 0.05$). Total PSP toxin content did not vary significantly between the strains, but differences in the amounts of PSP toxin analogues were observed (Fig. 1c, Fig. S1). For instance, AON5.26 contained more STX than the other two strains, consisting of 3.2% of the total PSP toxin content against 2.1% and 2.4% for AON13 and AON15, respectively (Fig. S2; $P < 0.001$). Total cellular toxicity also differed between the strains, with AON15 being significantly more toxic than the other two strain ($P < 0.05$), with averages of 4.6, 7.9 and 6.0 $\text{pg STXeq cell}^{-1}$, for AON13, AON15 and AON5.26, respectively (Fig. 1d).

There were also some differences in elemental composition. AON13 contained more POC and PON than AON15 and AON5.26, with averages of 306 against 228 and 192 pmol C cell^{-1} , and 40 against 32 and 27 pmol N cell^{-1} , respectively (Fig. 2a, b; $P < 0.05$). AON13 also had a significantly higher than C:P ratio than the other two strains (Table 2). However, there were no significant differences in cell volume (Table 2).

Untargeted analysis of VOCs also revealed differences in the production of VOCs between the strains under ambient CO₂ conditions. Different mass traces of VOCs were produced by the strains, where the volatilomes of AON15 and AON5.26 were quite similar as compared to the volatilome of AON13, which is illustrated by the separation based on PLS-DA (Fig. 3). Component 1 and 2 both do not clearly separate VOCs produced by AON15 and AON5.26.

3.3. Comparison between CO₂ treatments

Both AON15 and AON5.26 showed a significant increase in growth rate in response to CO₂ (Fig. 1a; $P < 0.01$). Only AON15 showed a decrease in all toxin quotas (PSP, GYM and SPX) and in overall toxicity in response to elevated $p\text{CO}_2$ ($P < 0.01$; Fig. 1b-d), while STX content decreased in both AON15 and AON5.26 (Fig. S2; $P < 0.05$). In contrast, PON and POC content, and POC production only increased in both AON13 and AON5.26 ($P < 0.001$), while all strains increased their PON

production (Fig. 2; $P < 0.01$). In AON5.26, C:P ratios showed a significant increase, while N:P ratios increased for both AON5.26 and AON15 ($P < 0.05$; Table 2). ϵ_p values only increased significantly for AON15 ($P < 0.01$; Table 1). Across strains, ϵ_p values increased with CO₂ concentration (Fig. 4a). Moreover, when corrected for C demand, ϵ_p showed a negative hyperbolic relationship with POC production/[CO₂] (i.e. ¹³C fractionation increased when C demand over supply was low, and vice versa), though with a lower correlation coefficient (Fig. 4b).

Elevated $p\text{CO}_2$ also caused a change in VOC production in all strains, illustrated by the separation in volatilomes based on partial least squares discriminant analysis (Fig. 3). Blends of VOCs produced by AON15 and AON5.26 showed a stronger shift with elevated CO₂ than those produced by AON13 (based on the most explanatory component). With more CO₂, AON13 was still more different in its volatilome as compared to AON15 and AON5.26, although this difference decreased based on the most explanatory component 1. We observed clear changes in up- and downregulation of mass traces of VOCs with elevated $p\text{CO}_2$ (Fig. 5), with the highest number of mass traces (53) being upregulated in strain AON13 and down-regulated (132) in strain AON15.

We also tested whether strains responded differently to elevated $p\text{CO}_2$ for each trait and found that AON5.26 exhibited a stronger increase in growth, and PON and POC content and production than both AON13 and AON15 (Fig. 1a, 2). On the other hand, AON15 showed a stronger decrease in toxicity and cyclic imine toxin content than the other two strains, and a significant stronger decrease in PSP toxin content than AON13 (Fig. 1b-d). In STX quotas, both AON15 and AON5.26 showed a comparable decrease in response to CO₂, while this was not the case for AON13 (Fig. S2).

4. Discussion

Elevated $p\text{CO}_2$ affected multiple phenotypic traits of the tested *A. ostentfeldii* strains, with general increases in growth rate, POC and PON content, and ϵ_p values, although not always significant. The strength of these trait responses varied between strains, while for other traits, such as toxin content, both the strength and direction of response varied between strains with no consistent response to elevated $p\text{CO}_2$.

4.1. Experimental setup

Over the course of the experiment, pH drift did occur as a result of biomass build-up (Table 1; compare $p\text{CO}_2$ with CO₂ treatment). In nature, pH and $p\text{CO}_2$ may vary substantially during the formation of an algal bloom, with severe reductions in CO₂ concentrations and associated increases in pH at the peak of a bloom (Hansen, 2002). It is unclear whether cells become limited by low CO₂ or inhibited by high pH in course of the experiment (Flynn et al., 2015; Hansen et al., 2007). Yet, by allowing some pH drift to occur, the experiment does represent changes in carbonate chemistry as result of biomass build-up under ambient and elevated CO₂ conditions, which also occurs naturally (Hansen, 2002), especially since the experimental cell densities are in the same order of magnitude as natural bloom densities (Brandenburg

Table 1

Carbonate chemistry and ¹³C fractionation (ϵ_p) for the different CO₂ treatments per strain, showing the mean over the course of the experiment. Values for DIC, pH and ϵ_p indicate the mean of triplicate incubations and $p\text{CO}_2$ was calculated based on pH and DIC of each incubation, using equilibrium constants by Mehrbach et al. (1973), refitted by Dickson and Millero (1987). Significance levels for $p\text{CO}_2$ and ϵ_p between the low and high CO₂ treatments are indicated by the asterisk (** $P < 0.01$, *** $P < 0.001$).

Strain	CO ₂ treatment	pH		DIC ($\mu\text{mol L}^{-1}$)		$p\text{CO}_2$ (μatm)		ϵ_p (‰)	
		mean	sd	mean	sd	mean	sd	mean	sd
AON13	400	8.23	0.02	1188	14	213	11	1.39	1.34
AON13	1000	7.82	0.01	1168	56	527***	30	11.17	5.30
AON15	400	8.07	0.07	1120	21	357	36	5.92	1.97
AON15	1000	7.75	0.08	1117	10	676***	55	15.42**	7.09
AON5.26	400	8.17	0.05	1085	15	286	13	6.21	1.23
AON5.26	1000	7.86	0.03	1126	2	479***	18	11.08	2.77

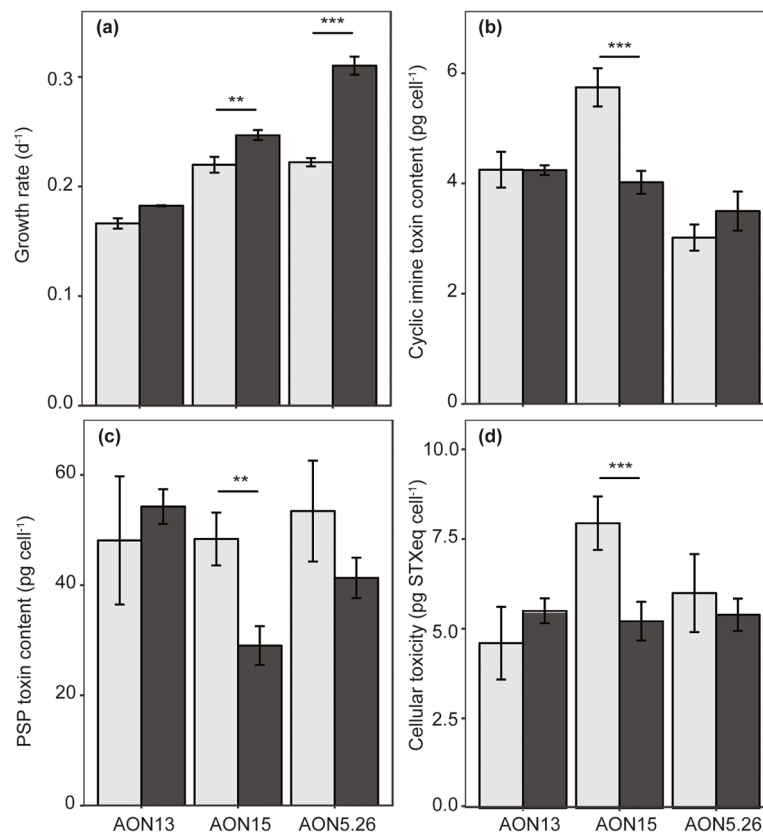


Fig. 1. a) growth rate, b) cyclic imine toxin, c) PSP toxin content and d) cellular toxicity content of the three strains in the low (light gray) and high (dark gray) CO₂ treatments ($n = 3$). Significance level is indicated by the asterisks (** $P < 0.01$, *** $P < 0.001$).

et al., 2017).

4.2. C and N assimilation

Strains tended to increase their growth rate in response to elevated $p\text{CO}_2$, although the strength of the response varied. The growth rate of AON13 showed a minor but insignificant increase, whereas the growth rates of AON15 and AON5.26 both showed a clear significant increase (Fig. 1a). There was also an overall increase in POC and PON quotas, and together with higher growth rates, this resulted in a higher POC and PON production with more CO₂ ($P < 0.05$; Fig. 2). Higher POC and PON quotas could be associated with larger cells, but there was no consistent increase in POP quota and cell volume (Table 2). This suggests that *A. ostenfeldii* cells increased both their C and N assimilation with elevated $p\text{CO}_2$, which may be explained by the close coupling of these respective assimilation pathways (Flynn, 1991; Turpin, 1991). A similar increase in C and N assimilation in response to more CO₂ was found in *A. fundyense*, although this experiment was performed under N-limiting conditions (Eberlein et al., 2016). Higher POC production rates may imply that strains were C limited in the ambient treatment and/or that strains could downscale their CCMs in the high CO₂ treatment and reallocate energy towards growth and C assimilation (Hoins et al., 2016).

4.3. CCM regulation

¹³C fractionation increased with elevated $p\text{CO}_2$ (Fig. 4a), although only specifically for AON15 (Table 1). Higher CO₂ concentrations allow RubisCO to better express its preference for ¹²C by acquiring more CO₂ relative to HCO₃⁻. It thus seems that all three strains acquired more CO₂, relative to HCO₃⁻, which might reflect a down-regulation of CCMs (Rost et al., 2008; Hoins et al., 2016a; but see below).

Although we did not measure CCM activity in *A. ostenfeldii*, several other studies have revealed effective and flexible CCMs in various *Alexandrium* species (Eberlein et al., 2014; Hoins et al., 2015; Toulza et al., 2010; Van de Waal et al., 2014). It is therefore conceivable that *A. ostenfeldii* also possesses effective and adjustable CCMs. This apparent possession of CCMs is supported by the hyperbolic relationship between ϵ_p and POC production/[CO₂], describing the dependency of ϵ_p on both C demand (POC production) and supply (CO₂ concentration; Fig. 4b). ¹³C fractionation is higher when the C demand is low and the C supply high, as RubisCO can better discriminate against ¹³C under such conditions. When cells solely depend on diffusive CO₂ uptake, one would expect an inverse linear relationship between ϵ_p and POC production/[CO₂], as ϵ_p changes directly as a function of CO₂ supply or C demand (i.e. changes in growth rate or cell size). Consequently, any deviation from such an inverse linear relationship between ϵ_p and POC production/[CO₂] indicates that cells can alter their C uptake through operation of a CCM. However, the hyperbolic relationship between ϵ_p and POC production/[CO₂] was only apparent when looking at the population level (i.e. across strains and CO₂ treatments). This may be due to the inclusion of more data points covering a broader range of POC production/[CO₂], as comparable relationships have earlier been shown for single strains (Hoins et al., 2015). Moreover, the differences in ϵ_p between the strains may also point towards different CCM strategies. Such an intraspecific variation in CCMs has been reported earlier for cyanobacteria and diatoms (Sandrini et al., 2014; Shen et al., 2017). It is conceivable that the population as a whole will benefit from this variation, as it provides a broader range of inorganic C concentrations where the species can prevail.

Strains varied in their ϵ_p values at ambient CO₂ conditions, as well as in the strength of the shifts in ϵ_p with elevated $p\text{CO}_2$, particularly when corrected for the C demands (Fig. 4b). The differences in ϵ_p values between the strains could thus suggest variations in the mode of CCMs,

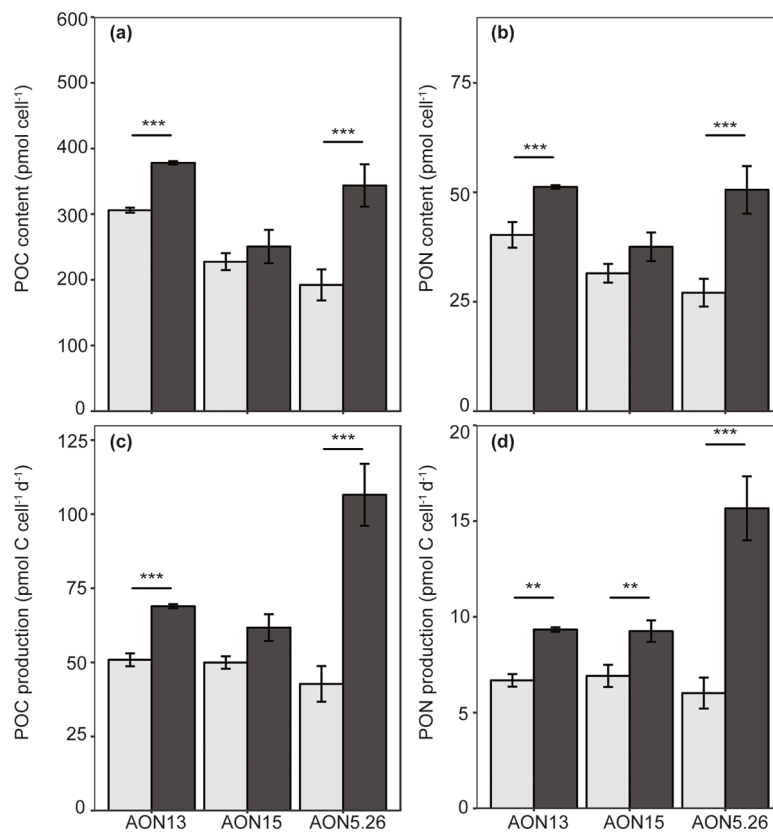


Fig. 2. a) POC content, b) PON content, c) POC production rate, and d) PON production rate of the three strains in the low (light gray) and high (dark gray) CO₂ treatments ($n = 3$). Significance level is indicated by the asterisks (** $P < 0.01$, *** $P < 0.001$).

Table 2

Cell volume and elemental ratios for the different CO₂ treatments per strain ($n = 3$). Significance levels between the low and high CO₂ treatments are indicated by the asterisk (* $P < 0.05$).

Strain	CO ₂ treatment	Cell volume ($\times 10^3 \mu\text{m}^3$)		C:N (molar)		C:P (molar)		N:P (molar)	
		mean	sd	mean	sd	mean	sd	mean	sd
AON13	400	216	19	7.6	0.6	96.2	14.0	12.7	2.8
AON13	1000	223	7	7.4	0.0	102.6	3.5	13.9	0.6
AON15	400	207	17	7.2	0.3	62.3	12.0	8.6	1.5
AON15	1000	202	31	6.7	0.1	92.6	25.4	13.9*	3.6
AON5.26	400	221	29	7.1	0.0	56.1	7.1	7.9	1.0
AON5.26	1000	232	22	6.8	0.1	90.0*	5.9	13.2*	1.0

where the relative contribution of HCO₃⁻ (which is ¹³C-enriched compared to CO₂) may be higher in AON13, or there may be less leakage (or less replenishment of the internal C pool). With elevated $p\text{CO}_2$, ϵ_p values increased for all strains, but the increase was not significant for AON5.26 and AON13. Also, when correcting for C demands (i.e. POC production), AON5.26 seems less sensitive due to a strong increase in POC production as well as weak changes in ϵ_p values with elevated $p\text{CO}_2$. This suggests intraspecific variation in the plasticity of CCMs, where AON5.26 was less able to adjust its CCM. Exactly which mode of CCMs *A. ostenfeldii* employs and if this can possibly vary between strains remains to be determined. However, an increase in relative CO₂ uptake, a downregulation of active C uptake and subsequent reallocation of energy would explain the observed increase in ϵ_p , growth and C assimilation.

4.4. Toxin production

PSP toxin quotas showed varying responses with elevated $p\text{CO}_2$ in the different strains. No significant change was observed for AON13 and AON5.26, while PSP toxins decreased with higher CO₂ in AON15.

Various responses of PSP toxins have been observed for different *Alexandrium* species and strains with increasing $p\text{CO}_2$ levels. In *A. fundyense* a decrease in toxin quotas, and particularly cellular toxicity was reported (Eberlein et al., 2016; Van de Waal et al., 2014). The latter was explained by a shift in sulfur metabolism with elevated $p\text{CO}_2$, as PSP toxin composition shifted from the toxic non-sulfated STX towards its less toxic sulfated analogues (Van de Waal et al., 2014). Non-sulfated STX and neoSTX are highly toxic, with LD₅₀ values (lethal dose for 50% of the population) in mice of approximately 8 $\mu\text{g kg}^{-1}$. Addition of a sulfate group in gonyautoxins (GTX) reduces toxicity by roughly 40%, and further addition of a sulfonyl group in C1/C2 toxins reduces toxicity by 99% (Wiese et al., 2010). In both AON15 and AON5.26, total STX quotas decreased with 30–60% in response to elevated $p\text{CO}_2$ (Fig. S2), but only in AON5.26 did the relative contribution of STX to the total toxin composition also decline (Fig. S1), which may point to a similar change in sulfur metabolism as observed for *A. fundyense*. Elevated $p\text{CO}_2$ can also positively affect toxicity, as was observed for *A. catenella* and several *A. ostenfeldii* strains from the Baltic Sea (Kremp et al., 2012; Tatters et al., 2013). These shifts were attributed to changes in toxin composition, with an increase in STX and GTX relative to C1/C2, which

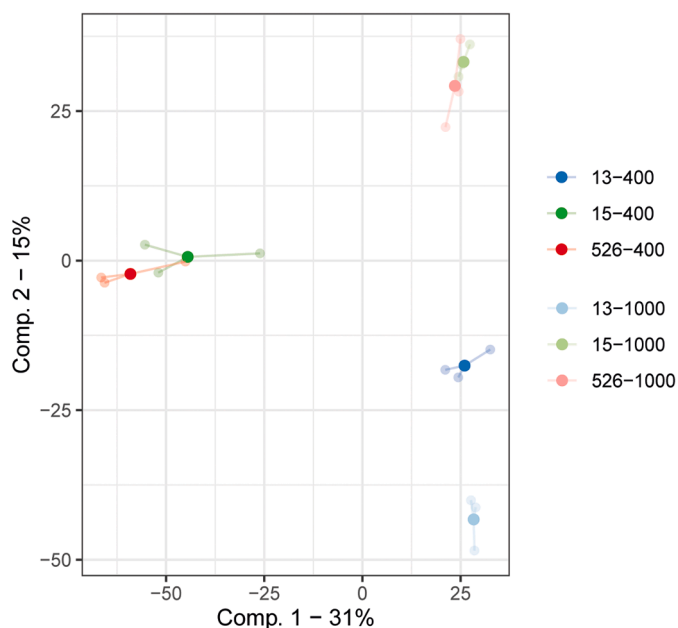


Fig. 3. Partial least squares discriminant analysis (PLS-DA) score plot of detected blends VOCs in all strains in both CO₂ treatments, where the replicates are connected with the centroid.

we also observed for AON15 (Fig. S1). Changes in CO₂ concentrations may thus cause differential shifts in toxicity though altered toxin composition. The exact mechanisms causing these shifts in PSP toxin composition, however, remain to be determined.

Cyclic imine toxin contents also decreased with elevated pCO₂ in AON15 (both SPX and GYM concentrations; Fig. 1b), while no changes were observed for the other two strains. These toxins are C-rich polyketides, and synthesis pathways of these compounds are closely coupled to cellular C acquisition (Staunton and Weissman, 2001). We therefore anticipated an increase in cyclic imine toxins with elevated pCO₂. A possible explanation for the lack of response or negative response could be the dilution effect through higher growth rates, preventing accumulation of toxins in the cells. AON15 contained more cyclic imine toxins than the other two strains, and this concentration decreased with more CO₂, possibly due to a higher growth rate. Indeed, when looking at

cyclic imine production rates, both AON13 and AON15 did not show a significant decrease and AON5.26 increased its cyclic imine production. Apparently, the synthesis of cyclic imine toxins is regulated largely independent of the availability of CO₂, which may result from the operation of effective CCMs allowing continuous fueling of C to downstream processes.

4.5. Volatile organic compounds

VOCs are compounds of low molecular weight with low to moderate hydrophilicity and high vapor pressures and low boiling points (Lemfack et al., 2013; Schmidt et al., 2015). Consequently, VOCs can easily diffuse through both air and water, allowing them to serve as potentially important infochemicals. There have been several studies on VOCs produced by phytoplankton, for instance on the production of volatile dimethyl sulfide (DMS) that can be released into the atmosphere and thereby influences large-scale meteorological processes (Gabric et al., 2001). Our untargeted VOC measurements indicate that the production of VOCs by *A. ostenfeldii* differs between strains (Fig. 3, 5). This can be

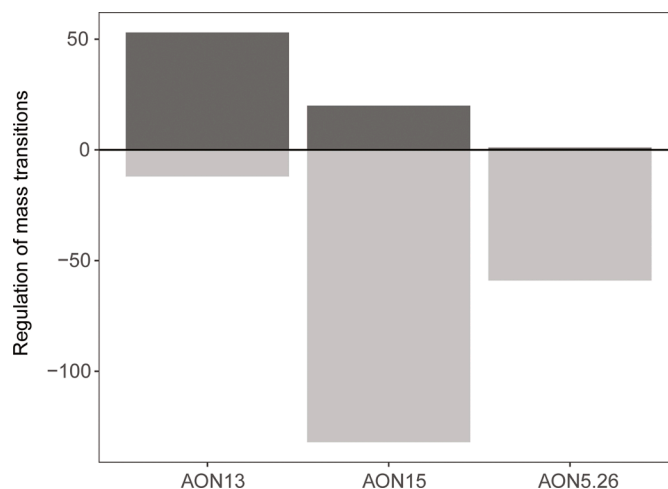


Fig. 5. Regulation of mass transitions in the three different strains in response to pCO₂, where positive numbers indicate an upregulation and negative numbers a downregulation.

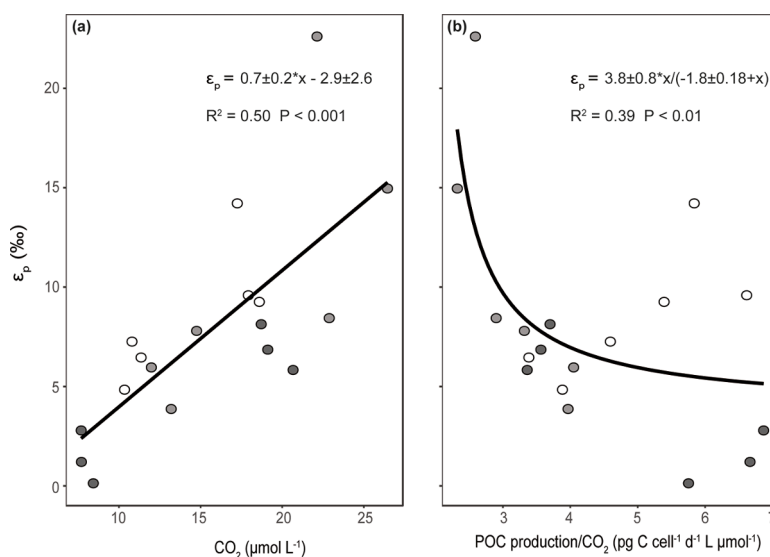


Fig. 4. ¹³C fractionation based on CO₂ of the three strains (AON13 is dark gray, AON15 is light gray, and AON5.26 is white) as a function of a) CO₂, and b) C demand over supply (POC production/[CO₂]). Trend lines represent the relationships between ¹³C fractionation and CO₂ (a) and POC production/[CO₂] (b).

due to the differences in growth rates and potential modes of CCMs that may thus affect C metabolism. Alternatively, the tested strains may also possess distinct microbiomes, which can alter the production of VOCs as well (Moore et al., 2020; Paul et al., 2013). There were no specific mass transitions found for all strains that were distinctly regulated, suggesting strain specific responses of the volatilome towards elevated $p\text{CO}_2$.

Although little is still known about the exact functions of VOCs and their modes of action (Schmidt et al., 2019, 2015), specifically in algae (Fink, 2007), intraspecific variation in the blends of VOCs released by *A. ostenfeldii* could suggest differences in cell to cell communication. Moreover, we also show that VOC production changes in response to higher CO_2 concentrations (Fig. 3), which may have implications for ecological functions depending on the role of these VOCs. Here, we performed an initial explorative study based on an untargeted VOC analysis, which already revealed intraspecific variation in volatilomes and their responses to $p\text{CO}_2$. Future research focusing on the identification of important algal VOCs, using a more targeted approach, are required to reveal the physiological processes underlying VOC synthesis. Understanding these processes may help to explain the observed intraspecific variation in the *A. ostenfeldii* volatilome, as well as the responses of the volatilome toward elevated $p\text{CO}_2$ and other climate change drivers.

4.6. Concluding remarks

Although the tested *A. ostenfeldii* strains are genetically very similar, they showed phenotypic variation within trait values (Brandenburg et al., 2018), as well as within trait responses towards elevated $p\text{CO}_2$. The intraspecific variation in trait responses to higher CO_2 availabilities was most pronounced in toxin content, which decreased for both PSP toxins and cyclic imines in AON15, AON5.26 showed changes in PSP toxin analogues, and toxins stayed largely unaltered in AON13. While all strains showed tentative increases in their growth rates and POC and PON production rates, we observed distinct differences in the strength of the responses between the strains. Traits appeared to be more plastic in strains AON5.26 and AON15 under elevated $p\text{CO}_2$ than in AON13, as growth rates increased the most in these strains and changes in the amount of toxins per cell were more pronounced. Consequently, AON5.26 and AON15 may thrive better under dynamic inorganic C conditions than AON13, for instance during bloom development with strong changes in CO_2 availabilities, while AON13 may be more specialized and thereby perform better under more stable inorganic C conditions, for instance during the period prior to a bloom.

Our findings are in line with other studies that showed considerable phenotypic variation in traits within algal populations (Alpermann et al., 2010; Burkholder and Glibert, 2006; Maranda et al., 1985), as well as differences in strain responses towards environmental stressors (Band-Schmidt et al., 2014; Kremp et al., 2012; Wang et al., 2006). Both standing phenotypic trait variation in populations and phenotypic plasticity in trait responses contribute to species resilience and adaptation towards changing environmental conditions (Litchman et al., 2012). *A. ostenfeldii* populations possess a high intraspecific trait variation (Brandenburg et al., 2018), and this coupled with considerable phenotypic plasticity in important functional traits, such as growth rate, may allow *Alexandrium* to rapidly adapt to changing environments.

Declaration of Competing Interest

The authors declare that they have no known competing financial interests or personal relationships that could have appeared to influence the work reported in this paper.

Acknowledgements

The authors thank Nico Helmsing for technical support and sample analyses. In addition, the authors thank Annegret Müller for analyses of

PSP toxins, and Arnold van Dijk (Utrecht University) for $\delta^{13}\text{C}$ DIC analyses. The authors also thank Hans Zweers for measuring VOCs on the GC-QTOF. The work of KB is funded by the Gieskes-Strijbis Foundation and the study was partially supported by the Helmholtz-Gemeinschaft Deutscher Forschungszentren through the research program PACES II of the Alfred Wegener Institut-Helmholtz Zentrum für Polar- und Meeresforschung. AS thanks the European Research Council for Consolidator Grant 771497.

Supplementary materials

Supplementary material associated with this article can be found, in the online version, at doi:10.1016/j.hal.2020.101970.

References

- Alpermann, T.J., Tillmann, U., Beszteri, B., Cembella, A.D., John, U., 2010. Phenotypic variation and genotypic diversity in a planktonic population of the toxic marine dinoflagellate *Alexandrium tamarense* (Dinophyceae). *J. Phycol.* 46, 18–32.
- Badger, M.R., Andrews, T.J., Whitney, S.M., Ludwig, M., Yellowlees, D.C., Leggat, W., Price, G.D., 1998. The diversity and coevolution of Rubisco, plastids, pyrenoids, and chloroplast-based CO_2 -concentrating mechanisms in algae. *Can. J. Bot.* 76, 1052–1071.
- Band-Schmidt, C.J., Bustillos-Guzmán, J.J., Hernández-Sandoval, F.E., Núñez-Vázquez, E.J., López-Cortés, D.J., 2014. Effect of temperature on growth and paralytic toxin profiles in isolates of *Gymnodinium catenatum* (Dinophyceae) from the Pacific coast of Mexico. *Toxicon* 90, 199–212.
- Barrett, R.D.H., Schluter, D., 2008. Adaptation from standing genetic variation. *Trends Ecol. Evol.* 23, 38–44.
- Beardall, J., Stojkovic, S., Larsen, S., 2009. Living in a high CO_2 world: impacts of global climate change on marine phytoplankton. *Plant Ecol. Divers.* 2, 191–205.
- Bolnick, D.I., Amarasekare, P., Aratju, M.S., Burger, R., Levine, J.M., Novak, M., Rudolf, V.H.W., Schreiber, S.J., Urban, M.C., Vasseur, D.A., 2011. Why intraspecific trait variation matters in community ecology. *Trends Ecol. Evol.* 26, 183–192.
- Borkman, D.G., Smayda, T.J., Tomas, C.R., York, R., Strangman, W., Wright, J.L.C., 2012. Toxic *Alexandrium peruvianum* (Balech and de Mendiola) Balech and Tangen in Narragansett Bay, Rhode Island (USA). *Harmful Algae* 19, 92–100.
- Brandenburg, K.M., Senerpont, L.N.De, Wohlrab, S., Krock, B., John, U., Van Scheppingen, Y., Van Donk, E., Van de Waal, D.B., 2017. Combined physical, chemical and biological factors shape *Alexandrium ostenfeldii* blooms in the Netherlands. *Harmful Algae* 63, 146–153.
- Brandenburg, K.M., Wohlrab, S., John, U., Kremp, A., Jerney, J., Krock, B., Van de Waal, D.B., 2018. Intraspecific trait variation and trade-offs within and across populations of a toxic dinoflagellate. *Ecol. Lett.* 21, 1561–1571.
- Bromke, M.A., Gialvalisco, P., Willmitzer, L., Hesse, H., 2013. Metabolic analysis of adaptation to short-term changes in culture conditions of the marine diatom *Thalassiosira pseudonana*. *PLoS ONE* 8, 1–11.
- Buchan, A., LeCleir, G.R., Gulvik, C.A., González, J.M., 2014. Master recyclers: features and functions of bacteria associated with phytoplankton blooms. *Nat. Rev. Microbiol.* 12, 686–698.
- Burkholder, J.M., Glibert, P.M., 2006. Intraspecific variability: an important consideration in forming generalisations about toxic algal species. *African J. Mar. Sci.* 28, 177–180.
- Burson, A., Matthijs, H.C.P., de Bruijne, W., Talens, R., Hoogenboom, R., Gerssen, A., Visser, P.M., Stomp, M., Steur, K., Van Scheppingen, Y., Huisman, J., 2014. Termination of a toxic *Alexandrium* bloom with hydrogen peroxide. *Harmful Algae* 31, 125–135.
- Cembella, A.D., Lewis, N.I., Quilliam, M.A., 2000. The marine dinoflagellate *Alexandrium ostenfeldii* (Dinophyceae) as the causative organism of spirolide shellfish toxins. *Phycologia* 39, 67–74.
- Charmantier, A., McCleery, R.H., Cole, L.R., Perrins, C., Kruuk, L.E.B., Sheldon, B.C., 2008. Adaptive phenotypic plasticity in response to climate change in a wild bird population. *Science* 320, 800–803.
- Dickson, A.G., Millero, F.J., 1987. A comparison of the equilibrium constants for the dissociation of carbonic acid in seawater media. *Deep. Res.* 34, 1733–1743.
- Doney, S.C., Fabry, V.J., Feely, R.A., Kleypas, J.A., 2009. Ocean acidification: the other CO_2 problem. *Ann. Rev. Mar. Sci.* 1, 169–192.
- Dutkiewicz, S., Morris, J.J., Follows, M.J., Scott, J., Levitan, O., Dyrman, S.T., Berman-Frank, I., 2015. Impact of ocean acidification on the structure of future phytoplankton communities. *Nat. Clim. Chang.* 5, 1002–1006.
- Eberlein, T., Van De Waal, D.B., Brandenburg, K.M., John, U., Voss, M., Achterberg, E.P., Rost, B., 2016. Interactive effects of ocean acidification and nitrogen limitation on two bloom-forming dinoflagellate species. *Mar. Ecol. Prog. Ser.* 543 <https://doi.org/10.3354/meps11568>.
- Eberlein, T., Van de Waal, D.B., Rost, B., 2014. Differential effects of ocean acidification on carbon acquisition in two bloom-forming dinoflagellate species. *Physiol. Plant.* 151, 468–479.
- Falkowski, P.G., Barber, R.T., Smetacek, V., 1998. Biogeochemical controls and feedbacks on ocean primary production. *Science* 281, 200–206.
- Fink, P., 2007. Ecological functions of volatile organic compounds in aquatic systems. *Mar. Freshw. Behav. Physiol.* 40, 155–168.

- Flynn, K.J., 1991. Algal carbon-nitrogen metabolism: a biochemical basis for modeling the interactions between nitrate and ammonium uptake. *J. Plankton Res.* 13, 373–387.
- Flynn, K.J., Clark, D.R., Mitra, A., Fabian, H., Hansen, P.J., Glibert, P.M., Wheeler, G.L., Stoeckle, D.K., Blackford, J.C., Brownlee, C., 2015. Ocean acidification with (de) eutrophication will alter future phytoplankton growth and succession. *Proc. R. Soc. B Biol. Sci.* 282.
- Freeman, H., Hayes, J.M., 1992. Fractionation of carbon isotopes by phytoplankton and estimates of ancient CO₂ levels. *Global Biogeochem. Cycles* 6, 185–198.
- Fu, F., Zhang, Y., Warner, M.E., Feng, Y., Sun, J., Hutchins, D.A., 2008. A comparison of future increased CO₂ and temperature effects on sympatric *Heterosigma akashiwo* and *Proocentrum minimum*. *Harmful Algae* 7, 76–90.
- Gabric, A., Gregg, W., Najjar, R., Erickson, D., Matrai, P., 2001. Modeling the biogeochemical cycle of dimethylsulfide in the upper ocean: a review. *Chemosph. - Glob. Chang. Sci.* 3, 377–392.
- Giordano, M., Beardall, J., Raven, J.A., 2005. CO₂ concentrating mechanisms in algae: mechanisms, environmental modulation, and evolution. *Annu. Rev. Plant Biol.* 56, 99–131.
- Godhe, A., Sjöqvist, C., Sildever, S., Seftom, J., Harðardóttir, S., Bertos-Fortis, M., Bunse, C., Gross, S., Johansson, E., Jonsson, P.R., Khandan, S., Legrand, C., Lips, I., Lundholm, N., Rengefors, K.E., Sassenhagen, I., Suikkanen, S., Sundqvist, L., Kremp, A., 2016. Physical barriers and environmental gradients cause spatial and temporal genetic differentiation of an extensive algal bloom. *J. Biogeogr.* 43, 1130–1142.
- Halsey, K.H., Giovannoni, S.J., Graus, M., Zhao, Y., Landry, Z., Thrash, J.C., Vergin, K.L., de Gouw, J., 2017. Biological cycling of volatile organic carbon by phytoplankton and bacterioplankton. *Limnol. Oceanogr.* 62, 2650–2661.
- Hansen, P.J., 2002. Effect of high pH on the growth and survival of marine phytoplankton: implications for species succession. *Aquat. Microb. Ecol.* 28, 279–288.
- Hansen, P.J., Lundholm, N., Rost, B., 2007. Growth limitation in marine red-tide dinoflagellates: effects of pH versus inorganic carbon availability. *Mar. Ecol. Prog. Ser.* 334, 63–71.
- Hausler, E.J., Dickhut, R.M., Falconer, R., Wozniak, A.S., 2013. Improved method for quantifying the air-sea flux of volatile and semi-volatile organic carbon. *Limnol. Oceanogr. Methods* 11, 287–297.
- Hoins, M., Eberlein, T., Großmann, C.H., Brandenburg, K., Reichart, G.-J., Rost, B., Sluijs, A., Van De Waal, D.B., 2016. Combined effects of ocean acidification and light or nitrogen availabilities on ¹³C fractionation in marine dinoflagellates. *PLoS ONE* 11.
- Hoins, M., Van de Waal, D.B., Eberlein, T., Reichart, G.J., Rost, B., Sluijs, A., 2015. Stable carbon isotope fractionation of organic cyst-forming dinoflagellates: evaluating the potential for a CO₂ proxy. *Geochim. Cosmochim. Acta* 160, 267–276.
- Hönisch, B., Ridgwell, A., Schmidt, D.N., Thomas, E., Gibbs, S.J., Sluijs, A., Zeebe, R., Kump, L., Martindale, R.C., Greene, S.E., Kiessling, W., Ries, J., Zachos, J.C., Royer, D.L., Barker, S., Marchitto, T.M., Moyer, R., Pelejero, C., Ziveri, P., Foster, G. L., Williams, B., 2012. The geological record of ocean acidification. *Science* 335, 1058–1063.
- Hooper, D.U., Chapin, F.S., Ewel, J.J., Hector, A., Inchausti, P., Lavorel, S., Lawton, J.H., Lodge, D.M., Loreau, M., Naeem, S., Schmid, B., Setälä, H., Symstad, A.J., Vandermeer, J., Wardle, D.A., 2005. Effects of biodiversity on ecosystem functioning: a consensus of current knowledge. *Ecol. Monogr.* 75, 3–35.
- Hurd, C.L., Beardall, J., Comeau, S., Cornwall, C.E., Havenhand, J.N., Munday, P.L., Parker, L.M., Raven, J.A., McGraw, C.M., 2020. Ocean acidification as a multiple driver: how interactions between changing seawater carbonate parameters affect marine life. *Mar. Freshw. Res.* 71, 263–274.
- Kallenbach, M., Veit, D., Eilers, E., Schuman, M., 2015. Application of silicone tubing for robust, simple, high-throughput, and time-resolved analysis of plant volatiles in field experiments. *Bio Protoc.* 5.
- Keller, M.D., Seluín, R.C., Claus, W., Guillard, R.R.L., 1987. Media for the culture of oceanic ultraphytoplankton. *J. Phycol.* 23, 633–638.
- Kremp, A., Godhe, A., Egardt, J., Dupont, S., Suikkanen, S., Casabianca, S., Penna, A., 2012. Intraspecific variability in the response of bloom-forming marine microalgae to changed climate conditions. *Ecol. Evol.* 2, 1195–1207.
- Kremp, A., Lindholm, T., Dressler, N., Erler, K., Gerds, G., Eirtovaara, S., Leskinen, E., 2009. Bloom forming *Alexandrium ostenfeldii* (Dinophyceae) in shallow waters of the Åland Archipelago, Northern Baltic Sea. *Harmful Algae* 8, 318–328.
- Krock, B., Sequel, C.G., Cembella, A.D., 2007. Toxin profile of *Alexandrium catenella* from the Chilean coast as determined by liquid chromatography with fluorescence detection and liquid chromatography coupled with tandem mass spectrometry. *Harmful Algae* 6 (5), 734–744.
- Lawson, C.A., Possell, M., Seymour, J.R., Raina, J.B., Suggett, D.J., 2019. Coral endosymbionts (Symbiodiniaceae) emit species-specific volatiles that shift when exposed to thermal stress. *Sci. Rep.* 9, 1–11.
- Lemfack, M.C., Nickel, J., Dunkel, M., Preissner, R., Piechulla, B., 2013. mVOC: a database of microbial volatiles. *Nucleic Acids Res.* 42, 744–748.
- Lenth, R., Buerkner, P., Herve, M., Love, J., Riebl, H., Singmann, H., 2020. emmeans: Estimated Marginal Means, Aka Least-Squares Means.
- Litchman, E., Edwards, K.F., Klausmeier, C.A., Thomas, M.K., 2012. Phytoplankton niches, traits and eco-evolutionary responses to global environmental change. *Mar. Ecol. Prog. Ser.* 470, 235–248.
- Maranda, L., Anderson, D.M., Shimizu, Y., 1985. Comparison of toxicity between populations of *Gonyaulax tamarensis* of Eastern North American water. *Estuar. Coast. Shelf Sci.* 21, 401–410.
- Medlin, L.K., Lange, M., Nothig, E., 2000. Genetic diversity in the marine phytoplankton: a review and a consideration of Antarctic phytoplankton. *Antarct. Sci.* 12, 325–333.
- Mehrbach, C., Culbertson, C.H., Hawley, J.E., Pytkowicz, R.M., 1973. Measurement of the apparent dissociation constants of carbonic acid in seawater at atmospheric pressure. *Limnol. Oceanogr.* 18, 897–907.
- Mook, W.G., Bommeron, J.C., Staverman, W.H., 1974. Carbon isotope fractionation between dissolved bicarbonate and gaseous carbon dioxide. *Earth Planet. Sci. Lett.* 22, 169–176.
- Moore, E.R., Davie-Martin, C.L., Giovannoni, S.J., Halsey, K.H., 2020. Pelagibacter metabolism of diatom-derived volatile organic compounds imposes an energetic tax on photosynthetic carbon fixation. *Environ. Microbiol.* 22, 1720–1733.
- Morriën, E., Hannula, S.E., Snoek, L.B., Helmsing, N.R., Zweers, H., De Hollander, M., Soto, R.L., Bouffaud, M.L., Buée, M., Dimmers, W., Duyts, H., Geisen, S., Girlanda, M., Griffiths, R.L., Jørgensen, H.B., Jensen, J., Plassart, P., Redecker, D., Schmelz, R.M., Schmidt, O., Thomson, B.C., Tisserant, E., Uroz, S., Winding, A., Bailey, M.J., Bonkowski, M., Faber, J.H., Martin, F., Lemanceau, P., De Boer, W., Van Veen, J.A., Van Der Putten, W.H., 2017. Soil networks become more connected and take up more carbon as nature restoration progresses. *Nat. Commun.* 8.
- Morse, D., Salois, P., Markovic, P., Hastings, J.W., 1995. A nuclear-encoded form II RubisCO in dinoflagellates. *Science* 268, 1622–1624.
- Nicotra, A.B., Atkin, O.K., Bonser, S.P., Davidson, A.M., Finnegan, E.J., Mathesius, U., Poot, P., Purugganan, M.D., Richards, C.L., Valladares, F., Van Kleunen, M., 2010. Plant phenotypic plasticity in a changing climate. *Trends Plant Sci.* 15, 684–692.
- Paul, C., Mausz, M.A., Pohnert, G., 2013. A co-culturing/metabolomics approach to investigate chemically mediated interactions of planktonic organisms reveals influence of bacteria on diatom metabolism. *Metabolomics* 9, 349–359.
- Pierrot, D.E., Lewis, E., Wallace, D.W.R., 2006. Program developed for CO₂ system calculations.
- Post, W.M., Peng, T., Emanuel, W.R., King, A.W., Dale, V.H., DeAngelis, D.L., 1990. The global carbon cycle. *Am. Sci.* 78, 310–326.
- R Core Team, 2018. R: a language and environment for statistical computing.**
- Ratti, S., Giordano, M., Morse, D., 2007. CO₂-concentrating mechanisms of the potentially toxic dinoflagellate *Protoceratium reticulatum* (Dinophyceae, Gonyaulacales). *J. Phycol.* 43, 693–701.
- Reinfelder, J.R., 2011. Carbon concentrating mechanisms in eukaryotic marine phytoplankton. *Ann. Rev. Mar. Sci.* 3, 291–315.
- Riebesell, U., Kortzinger, A., Oschlies, A., 2009. Sensitivities of marine carbon fluxes to ocean change. *Proc. Natl. Acad. Sci.* 106, 20602–20609.
- Rohart, F., Gautier, B., Singh, A., Le Cao, K.A., 2017. mixOmics: an R package for 'omics feature selection and multiple data integration. *PLoS Comput. Biol.* 13, e1005752.
- Rost, B., Richter, K., Riebesell, U., Hansen, P.J., 2006. Inorganic carbon acquisition in red tide dinoflagellates. *Plant. Cell Environ.* 29, 810–822.
- Rost, B., Zondervan, I., Wolf-Gladrow, D., 2008. Sensitivity of phytoplankton to future changes in ocean carbonate chemistry: current knowledge, contradictions and research directions. *Mar. Ecol. Prog. Ser.* 373, 227–237.
- Ruiz-Halpern, S., Sejir, M.K., Duarte, C.M., Krause-Jensen, D., Dalsgaard, T., Dachs, J., Rysgaard, S., 2010. Air-water exchange and vertical profiles of organic carbon in a subarctic fjord. *Limnol. Oceanogr.* 55, 1733–1740.
- Sandrini, G., Matthijs, H.C.P., Verspagen, J.M.H., Muyzer, G., Huisman, J., 2014. Genetic diversity of inorganic carbon uptake systems causes variation in CO₂ response of the cyanobacterium *Microcystis*. *ISME J* 8, 589–600.
- Schmidt, R., Cordovez, V., De Boer, W., Raaijmakers, J., Garbeva, P., 2015. Volatile affairs in microbial interactions. *ISME J* 9, 2329–2335.
- Schmidt, R., Ulanova, D., Wick, L.Y., Bode, H.B., Garbeva, P., 2019. Microbe-driven chemical ecology: past, present and future. *ISME J* 13, 2656–2663.
- Schulz-Bohm, K., Zweers, H., de Boer, W., Garbeva, P., 2015. A fragrant neighborhood: volatile mediated bacterial interactions in soil. *Front. Microbiol.* 6, 1212e.
- Shen, C., Dupont, C.L., Hopkinson, B.M., 2017. The diversity of CO₂-concentrating mechanisms in marine diatoms as inferred from their genetic content. *J. Exp. Bot.* 68, 3937–3948.
- Shiojiri, K., Kishimoto, K., Ozawa, R., Kugimiya, S., Urashimo, S., Arimura, G., Horiuchi, J., Nishioka, T., Matsui, K., Takabayashi, J., 2006. Changing green leaf volatile biosynthesis in plants: an approach for improving plant resistance against both herbivores and pathogens. *Proc. Natl. Acad. Sci. U. S. A.* 103, 16672–16676.
- Staunton, J., Weissman, K.J., 2001. Polyketide biosynthesis: a millennium review. *Nat. Prod. Rep.* 18, 380–416.
- Stocker, T.F., Qin, D., Plattner, G.K., Tignor, M., Allen, S.K., Boschung, J., Nauels, A., Xia, Y., Bex, V., Midgley, P.M., 2013. Climate Change 2013 - The Physical Science Basis. Working Group I Contribution to the Fifth Assessment Report of the Intergovernmental Panel On Climate Change. Cambridge University Press, Cambridge, UK.
- Sunda, W.G., Kieber, D., Kiene, R.P., 2002. An antioxidant function of DMSP and DMS in marine algae oceanic dimethylsulfide (DMS) photolysis. *Nature* 418, 317–320.
- Tatters, A.O., Flewelling, L.J., Fu, F., Granholm, A.A., Hutchins, D.A., 2013. High CO₂ promotes the production of paralytic shellfish poisoning toxins by *Alexandrium catenella* from Southern California waters. *Harmful Algae* 30, 37–43.
- Thoms, S., Pahlow, M., Wolf-Gladrow, D.A., 2001. Model of the carbon concentrating mechanism in chloroplasts of eukaryotic algae. *J. Theor. Biol.* 208, 295–313.
- Tomas, C.R., Van Wagoner, R., Tatters, A.O., White, K.D., Hall, S., Wright, J.L.C., 2012. *Alexandrium peruvianum* (Balech and Mendiola) Balech and Tangen a new toxic species for coastal North Carolina. *Harmful Algae* 17, 54–63.
- Toulza, E., Shin, M.S., Blanc, G., Audic, S., Laabir, M., Collos, Y., Claverie, J.M., Grzebyk, D., 2010. Gene expression in proliferating cells of the dinoflagellate *Alexandrium catenella* (Dinophyceae). *Appl. Environ. Microbiol.* 76, 4521–4529.
- Turpin, D.H., 1991. Effects of inorganic N availability on algal photosynthesis and carbon metabolism. *J. Phycol.* 27, 14–20.
- Tyc, O., Zweers, H., de Boer, W., Garbeva, P., 2015. Volatiles in inter-specific bacterial interactions. *Front. Microbiol.* 6, 1412.

- Van de Waal, D.B., Brandenburg, K.M., Keuskamp, J., Trimborn, S., Rokitta, S., Kranz, S., Rost, B., 2019. Highest plasticity of carbon concentrating mechanisms in earliest evolved phytoplankton. *Limnol. Oceanogr. Lett.* 4, 37–43.
- Van de Waal, D.B., Eberlein, T., John, U., Wohlrab, S., Rost, B., 2014. Impact of elevated pCO₂ on paralytic shellfish poisoning toxin content and composition in *Alexandrium tamarense*. *Toxicon* 78, 58–67.
- Van de Waal, D.B., Litchman, E., 2020. Multiple global change stressor effects on phytoplankton nutrient acquisition in a future ocean. *Philos. Trans. R. Soc. B* 375, 1–8.
- Van de Waal, D.B., Tillmann, U., Martens, H., Krock, B., Van Scheppingen, Y., John, U., 2015. Characterization of multiple isolates from an *Alexandrium ostenfeldii* bloom in The Netherlands. *Harmful Algae* 49, 94–104.
- Violle, C., Enquist, B.J., McGill, B.J., Jiang, L., Hulshof, C., Jung, V., Messier, J., 2012. The return of the variance: intraspecific variability in community ecology. *Trends Ecol. Evol.* 27, 244–252.
- Wang, D.Z., Zhang, S.G., Gu, H.F., Lai Chan, L., Hong, H.S., 2006. Paralytic shellfish toxin profiles and toxin variability of the genus *Alexandrium* (Dinophyceae) isolated from the Southeast China Sea. *Toxicon* 48, 138–151.
- Wiese, M., D'Agostino, P.M., Mihali, T.K., Moffitt, M.C., Neilan, B.A., 2010. Neurotoxic alkaloids: saxitoxin and its analogs. *Mar. Drugs* 8, 2185–2211.
- Xia, J., Sinelnikov, I.V., Han, B., Wishart, D.S., 2015. MetaboAnalyst 3.0-making metabolomics more meaningful. *Nucleic Acids Res* 43, W251–W257.
- Zeebe, R.E., Wolf-Gladrow, D.A., 2001. CO₂ in Seawater: Equilibrium, Kinetics, Isotopes. Elsevier Science Publishing Co., Amsterdam, the Netherlands.
- Zhang, J., Quay, P.D., Wilbur, D.O., 1995. Carbon isotope fractionation during gas-water exchange and dissolution of CO₂. *Geochim. Cosmochim. Acta* 59, 107–114.
- Zuo, Z., 2019. Why algae release volatile organic compounds - The emission and roles. *Front. Microbiol.* 10, 1–7.